Techno-economic analysis of forward osmosis pre-concentration before an anaerobic membrane bioreactor: Impact of draw solute and membrane material

Sergi Vinardell, Gaetan Blandin, Federico Ferrari, Geoffroy Lesage, Joan Mata-Alvarez, Joan Dosta, Sergi Astals

Techno-economic analysis of forward osmosis pre-concentration before an anaerobic membrane bioreactor: Impact of draw solute and membrane material

Sergi Vinardell[a,*], Gaetan Blandin[b], Federico Ferrari[c], Geoffroy Lesage[d], Joan Mata-Alvarez[a,e], Joan Dosta[a,e], Sergi Astals[a]

[a] Department of Chemical Engineering and Analytical Chemistry, University of Barcelona, 08028, Barcelona, Spain

[b] Laboratory of Chemical and Environmental Engineering (LEQUiA), Institute of the Environment, University of Girona, 17003, Girona, Spain

[c] Eurecat, Centre Tecnològic de Catalunya, Water, Air and Soil Unit, 08242, Manresa, Spain

[d] Institut Européen des Membranes (IEM), Université de Montpellier, CNRS, ENSCM, 34090, Montpellier, France

[e] Water Research Institute, University of Barcelona, 08028, Barcelona, Spain

*Corresponding author (svinardell@ub.edu)

Abstract

This research investigated the impact of draw solute and membrane material on the economic balance of a forward osmosis (FO) system pre-concentrating municipal sewage prior to an anaerobic membrane bioreactor (AnMBR). Eight and three different draw solutes were evaluated for cellulose triacetate (CTA) and polyamide thin film composite (TFC) membranes, respectively. The material of the FO membrane was a key economic driver since the net cost of TFC membrane was substantially lower than the CTA membrane. The draw solute had a moderate impact on the economic balance. The most economically favourable draw solutes were sodium acetate and calcium chloride for the CTA membrane and magnesium chloride for the TFC membrane. The FO+AnMBR performance was modelled for both FO membrane materials and each draw solute considering three FO recoveries (50, 80 and 90%). The estimated COD removal efficiency of the AnMBR was similar regardless of the draw solute and FO membrane material. However, the COD and draw solute concentrations in the permeate and digestate increased as the FO recovery increased. These results highlight that FO membranes with high permselectivity are needed to improve the economic balance of mainstream AnMBR and to ensure the quality of the permeate and digestate.

Keywords

Forward osmosis (FO); Anaerobic membrane bioreactor (AnMBR); Anaerobic digestion; Reverse osmosis (RO); Draw solute; Techno-economic evaluation

1. Introduction

Climate change and resource depletion are pushing a paradigm shift in wastewater treatment plants (WWTPs) to maximise the recovery of resources and reduce the consumption of chemicals and energy (Zhang and Liu, 2022). In this new paradigm, membrane bioreactors play a central role since these technologies provide a physical barrier for solids and pathogens, which allows producing high-quality effluents and improving the performance of the bioreactor (Krzeminski et al., 2017).

Anaerobic membrane bioreactor (AnMBR), which combines membrane technology and anaerobic digestion, is an interesting biotechnology for municipal sewage treatment (Vinardell et al., 2020b). In AnMBRs, the sewage organic matter is transformed into methane-rich biogas and the biomass is completely retained by the membrane (Anjum et al., 2021; Hu et al., 2021). Several full-scale AnMBRs have already been implemented for the treatment of different types of industrial wastewater (Zhen et al., 2019). However, full-scale implementation of AnMBRs for municipal sewage treatment is limited because municipal sewage is typically less concentrated and represents a larger volumetric flow rate than industrial wastewater. The high volumetric flow rate and the low organic matter concentration of municipal sewage: (i) increases the AnMBR capital and operating costs, (ii) decreases the methane productivity per m^3 of sewage, and (iii) increases the total amount of methane dissolved in the effluent (Ferrari et al., 2019; Zahedi et al., 2021). Accordingly, it is important to develop technologies for sewage pre-concentration to improve the competitiveness of AnMBR for municipal sewage treatment.

Forward osmosis (FO) is an emerging membrane technology to pre-concentrate municipal sewage with low energy input, low fouling and high rejection of organic matter

(Awad et al., 2019; Wang and Liu, 2021). FO is spontaneously driven by the osmotic pressure difference between the feed solution and the saline draw solution (Blandin et al., 2021). The osmotic pressure gradient between both solutions drives the permeation of water from the feed solution to the draw solution through the dense FO membrane (Almoalimi and Liu, 2022). The most used materials for FO membranes are cellulose triacetate (CTA) and polyamide thin film composite (TFC) (Kim et al., 2022). The application of FO pre-concentration allows increasing the sewage organic matter concentration and decreasing the volumetric flow rate (Ansari et al., 2017). Moreover, a regeneration technology (e.g. reverse osmosis (RO), nanofiltration, membrane distillation) is typically used to re-concentrate the draw solution and produce high-quality water from the diluted draw solution (Cabrera-Castillo et al., 2021; Kim et al., 2017). The combination of FO, RO and AnMBR technologies for municipal sewage treatment can provide potential economic advantages in comparison with typical WWTP configurations (Vinardell et al., 2020a).

Draw solute selection is important since it affects the water and solute fluxes through FO membranes (Ansari et al., 2015; Arcanjo et al., 2020). Small inorganic solutes (e.g. NaCl, KCl) have been widely used as draw solutes because they feature high diffusivities and mitigate the detrimental effect of internal concentration polarisation (ICP) on water flux (Lutchmiah et al., 2014; Shaffer et al., 2015). However, these solutes generally feature high reverse solute fluxes (RSF) due to their high diffusivity (Zou et al., 2019). The RSF from the draw to the feed solution: (i) increases the salinity of the sewage and (ii) increases the draw solution replenishment costs (Ferby et al., 2020). The higher salinity in the pre-concentrated sewage could partially inhibit anaerobic bacteria with a direct impact on the AnMBR biogas production and effluent quality (both permeate and

digestate) (Vinardell et al., 2021). Therefore, the selection of the draw solute should contemplate both FO and AnMBR performance since solute selection can have a high impact on the technical and economic feasibility of combining both technologies.

Few studies have evaluated the impact of the draw solute on FO and anaerobic digestion performance (Ansari et al., 2015; Bacaksiz et al., 2021). Bacaksiz et al. (2021) evaluated the performance of different inorganic and organic draw solutes in the FO system and the inhibitory impact of these solutes on anaerobic digestion. The authors showed that the draw solute has a direct impact on the water flux and RSF of the CTA-FO membrane. Anaerobic digestion batch experiments showed that the RSF of inorganic draw solutes could inhibit the anaerobic digestion process, while organic draw solutes could increase methane production. Finally, Bacaksiz et al. (2021) conducted a preliminary economic analysis and reported that $CaCl_2$, $MgCl_2$, HCOONa and CH_3COONa were the most economically favourable draw solutes. However, the economic analysis only included the draw solute purchase cost, but did not include all the capital, operating costs and revenue (e.g. FO installation, labour, maintenance, membrane replacement, electricity production) influenced by the draw solute and FO membrane material. To the best of the authors' knowledge, the combined impact of draw solute and FO membrane material on the economic balance of a system combining FO and AnMBR technologies has not yet been evaluated. Accordingly, a detailed techno-economic analysis is needed to understand how these factors influence the economic feasibility of an FO+AnMBR system for municipal sewage treatment.

The main objective of this study is to evaluate the impact of draw solute and FO membrane material on the economic balance of an FO+AnMBR system for municipal sewage treatment. To this end, two FO membrane materials (CTA and TFC) and eight

different draw solutes (NaCl, $MgCl_2$, KCl, $CaCl_2$, Na_2SO_4, $MgSO_4$, $Ca(NO_3)_2$ and CH_3COONa) were considered for the techno-economic analysis.

2. Methodology

2.1 Design criteria and draw solutes selection

Figure 1 shows the FO+AnMBR configuration evaluated in this study. The chosen configuration was a closed-loop scheme using a synthetic solution as a draw solution. The diluted draw solution was regenerated by means of RO to re-establish the initial osmotic pressure and to produce high-quality water. The draw solute was replenished (by topping up with salts) to keep the osmotic pressure constant in the loop despite losses of the draw solute through FO and RO membranes. The FO recovery was fixed at 80% because this is one of the most used FO recovery values in the literature for FO pre-concentration systems before anaerobic digestion (values range between 50 and 90%) (Ansari et al., 2018; Vinardell et al., 2021). The pre-concentrated municipal sewage was considered to be fed to an AnMBR configured as a continuous stirred tank reactor. The membranes were submerged in a separate membrane tank where gas sparging was applied to control the membrane fouling extent since this is the most common strategy for membrane fouling control in AnMBRs (Maaz et al., 2019). The AnMBR was considered to be operated at a solids retention time (SRT) of 60 days and at an hydraulic retention time (HRT) of 1 day (Vinardell et al., 2020a).

The selection of the draw solutes used for the economic evaluation was performed from available data for CTA and polyamide TFC commercial membranes. Regarding CTA membranes, seven inorganic and one organic draw solutes were evaluated: NaCl, $MgCl_2$, KCl, $CaCl_2$, Na_2SO_4, $MgSO_4$, $Ca(NO_3)_2$ and CH_3COONa (Achilli et al., 2010; Ansari et

al., 2015). Regarding TFC membranes, three different inorganic draw solutes were evaluated: NaCl, $MgCl_2$ and $MgSO_4$ (Sanahuja-Embuena et al., 2019). This research did not include the same draw solutes for both membranes due to the limited data available in the literature regarding draw solute permeability in TFC membranes. The osmotic pressure of the draw solution before entering to the FO modules was considered to be 28 bar for all the solutes, which is within the osmotic pressure range reported in previous studies (Achilli et al., 2010; Sanahuja-Embuena et al., 2019). The concentration of each draw solute at this osmotic pressure can be found in Table 1.

The economic analysis was conducted for a high-sized WWTP treating 100,000 m^3 d^{-1} of municipal sewage (500,000 population equivalent). The municipal sewage was pre-filtered (~50 μm) before FO to prevent substantial fouling and clogging in the FO membranes and to decrease the amount of suspended solids fed to the AnMBR. The pre-filtered municipal sewage contained a total chemical oxygen demand (COD) concentration of 420 mg COD L^{-1}, which was fractionated in biodegradable soluble COD (64.3%), inert soluble COD (19.1%), biodegradable particulate COD (7.1%) and inert particulate COD (9.5%) (Vinardell et al., 2020a).

2.2 FO process design and modelling

The water flux (J_W) and RSF (J_S) through dense FO membranes were modelled for all draw solutes and both membranes. Eq. (1) and Eq. (2) were used to model J_W and J_S, respectively (Tiraferri et al., 2013). These equations considered that the active layer faced the feed side and included the effect of (i) dilutive ICP on the support layer, (ii) concentrative external concentration polarisation (ECP) on the active layer and (iii) RSF from the draw solution to the sewage (Blandin et al., 2015).

$$J_W = A \cdot \left[\frac{\pi_D \cdot e^{-J_W \cdot \frac{S}{D}} - \pi_F \cdot e^{\frac{J_W}{k}}}{1 - \frac{B}{J_W} \cdot \left(e^{-J_W \cdot \frac{S}{D}} - e^{\frac{J_W}{k}} \right)} \right] \quad \text{Eq. (1)}$$

$$J_s = B \cdot \left[\frac{c_D \cdot e^{-J_W \cdot \frac{S}{D}} - c_F \cdot e^{\frac{J_W}{k}}}{1 + \frac{B}{J_W} \cdot \left(e^{\frac{J_W}{k}} - e^{-J_W \cdot \frac{S}{D}} \right)} \right] \quad \text{Eq. (2)}$$

where J_w is the water flux (L m^{-2} h^{-1}), J_S is the reverse draw solute flux (g m^{-2} h^{-1}), A is the water permeability (L m^{-2} h^{-1} bar^{-1}), B is the draw solute permeability (L m^{-2} h^{-1}), π_D is the osmotic pressure in the draw solution (bar), π_F is the osmotic pressure in the feed solution (bar), c_D is the draw solute concentration in the draw solution (g L^{-1}), c_F is the draw solute concentration in the feed solution (g L^{-1}), k is the mass transfer coefficient of the draw solute (L m^{-2} h^{-1}), D is the self-diffusion coefficient of the draw solute (L m^{-1} h^{-1}) and S is the membrane structural parameter (m). A, B and S parameters are widely used in FO research because they allow comparison of FO performance regardless of the operating conditions (Tiraferri et al., 2013).

The intrinsic membrane parameters (i.e. A and S) for CTA and TFC membranes were obtained from Coday et al. (2013) and Sanahuja-Embuena et al. (2019), respectively. The parameter B, which depends on both the membrane and the draw solute, was obtained from Achilli et al. (2010) and Ansari et al. (2015) for CTA membrane, and from Sanahuja-Embuena et al. (2019) for TFC membrane. In these publications, the CTA membrane was a commercial FO membrane from Hydration Technology Innovations (HTI) (Albany, USA) and the TFC membrane was a commercial FO membrane from Aquaporin (Kongens Lyngby, Denmark) (Sanahuja-Embuena et al., 2019). HTI CTA membrane and Aquaporin TFC membrane parameters A, B and S were chosen as they were available in the literature and are representative for commercial CTA and TFC membranes. Detailed

information about the A, B and S parameters as well as about the properties of the different draw solutes can be found in Table 1.

2.3 Modelling AnMBR performance

The AnMBR performance was modelled for the different FO alternatives (i.e. draw solutes, membrane materials and FO recoveries) to calculate the COD removal, the amount of methane recovered and the quality of the permeate. The presence of draw solute in the pre-concentrated sewage due to RSF could partially inhibit anaerobic biomass (i.e. Na^+, K^+, Ca^{2+}, Mg^{2+}), introduce an electron acceptor (i.e. SO_4^{2-} and NO_3^-) and/or introduce an electron donor (i.e. CH_3COO^-). The concentration of each draw solute in the AnMBR influent can be found in Table S1 of the supplementary information.

A steady state mass balance was used to model the AnMBR including a non-competitive inhibition function to determine the impact of draw solute concentration on anaerobic digestion performance (Eq. (3)). Subsequently, the total organic matter concentration in the AnMBR permeate was calculated using Eq. (4):

$$Q_0 \cdot S_{S,0} - k_{m,ac} \cdot \frac{S_S}{S_S + K_{S,ac}} \cdot \frac{KI_{50}}{KI_{50} + S_{cat}} X_{ac} \cdot V = Q_e \cdot S_S \qquad \text{Eq. (3)}$$

$$S_e = S_S + S_I \qquad \text{Eq. (4)}$$

where Q_0 is the pre-concentrated sewage flow rate ($m^3\ d^{-1}$), $S_{S,0}$ is the biodegradable organic matter (particulate and soluble) concentration in the pre-concentrated sewage (kg COD m^{-3}), $k_{m,ac}$ is the specific maximum uptake rate for acetogenic methanogens (kg COD kg^{-1} COD_{cell} d^{-1}), Ss is the soluble biodegradable organic matter concentration in the AnMBR and in the permeate (kg COD m^{-3}), $K_{S,ac}$ is the half-saturation constant for acetogenic methanogens (kg COD m^{-3}), KI_{50} is the 50% inhibitory constant for the draw

solute (kg COD m^{-3}), S_{cat} is the cation concentration (i.e. Na^+, K^+, Ca^{2+}, Mg^{2+}) of the draw solute in the AnMBR (kg COD m^{-3}), X_{ac} is the biomass concentration of acetogenic methanogens, which was considered to be a 10% of the biomass (kg COD_{cell} m^{-3}) (Ariesyady et al., 2007), V is the volume of the AnMBR (m^3), Q_e is the permeate flow rate (m^3 d^{-1}), S_e is the total soluble organic matter concentration in the AnMBR permeate (kg COD m^{-3}) and S_I is the soluble inert organic matter concentration in the influent (kg COD m^{-3}). The model parameters used in Eq. (3) can be found in Table S2~~1~~ of the supplementary material. Eq. (3) and Eq. (4) assumed that: (i) methanogenesis is the rate-limiting step, (ii) all the biodegradable particulate organic matter is solubilised in the AnMBR because of the high SRT (60 days), (iii) particulate organic matter hydrolysis does not generate soluble inert material, (iv) the AnMBR waste sludge flow rate is negligible compared to the permeate flow rate and (v) the KI_{50} values are literature averages and potential acclimation to inhibitors was not considered.

The methane production was calculated considering: (i) the biodegradable COD removed in the AnMBR, (ii) the presence of electron acceptors (i.e. SO_4^{2-} and NO_3^-) from the draw solution that could consume part of the COD, (iii) the presence of external COD coming from the draw solution (i.e. acetate) that could be an additional organic source for methane production and (iv) that a fraction on the methane remains dissolved in the effluent, which was calculated with Henry's law. It was considered that the organic matter consumed when sulphate and nitrate were contained in the pre-concentrated sewage corresponded to 2.01 mg COD mg^{-1} SO_4^{2-}-S and 2.86 mg COD mg^{-1} NO_3^--N, respectively (Metcalf & Eddy, 2014).

2.4 Costs and revenue calculation

223 Draw solution has a direct impact on the FO capital and operating costs since it affects
224 the water and the draw solute RSF through FO membranes. The RSF could also impact
225 the amount of methane recovered in the AnMBR and the quality of the permeate. This
226 section describes the costs and revenue considered for the economic evaluation. The cost
227 calculation was conducted considering a fixed FO recovery of 80% and a draw solution
228 osmotic pressure of 28 bar for all draw solutes and FO membrane materials (see Section
229 2.1). It is worth mentioning that the costs and revenue that were not influenced by the
230 draw solute or the FO membrane material were not considered for the economic
231 evaluation (e.g. AnMBR capital and operating costs, RO capital costs, energy
232 consumption, water production) since these costs and revenue are assumed to be similar
233 regardless of the draw solute and FO membrane material used. Table S3 of the
234 supplementary material shows detailed information about the parameters used for costs
235 and revenue calculations.

236 **2.4.1 FO capital and operating costs**

237 The methodology used to calculate the capital costs of the FO system can be found in
238 Vinardell et al. (2020a), who adapted the methodology proposed by Blandin et al. (2015)
239 to estimate the FO costs. Briefly, the capital costs of the FO system were estimated
240 considering relationships with capital costs of typical full-scale spiral wound RO systems
241 since (i) RO systems are rather similar to FO systems and (ii) there are more data available
242 concerning the costs of RO systems than FO systems (Blandin et al., 2015). Firstly, a
243 benchmark RO scenario was established, which corresponded to an RO installation
244 requiring a similar membrane area than the FO installation using NaCl as a draw solute.
245 The capital cost of the benchmark RO scenario was estimated (i) considering an RO
246 membrane cost of 21 € m^{-2} (Valladares Linares et al., 2016) and (ii) using the RO cost

distribution shown in Table S4~~3~~ of the supplementary material. Second, the capital cost of the FO system for the NaCl was estimated (i) considering an FO membrane cost of 55 £ m^{-2} (49 € m^{-2}) (Valladares Linares et al., 2016) and (ii) considering that specific cost contributors of the RO system could be partially (or totally) extendible to FO capital costs (e.g. civil engineering, equipment and materials, pumps) (Table S4~~3~~). Finally, the FO capital costs for all the other draw solute scenarios were calculated from the FO capital costs of the NaCl scenario and considering that specific cost contributors were dependent on the FO membrane area (Table S4~~3~~). The capital costs dependent on the FO membrane area were included in the economic evaluation since the costs that did not depend on the FO membrane area were not influenced by the draw solute and, therefore, are out of the scope of the present study.

The operating costs of the FO system accounted for membrane replacement, labour and maintenance. The membrane replacement cost was calculated assuming a membrane lifetime of 4 years (Yangali-Quintanilla et al., 2015). The labour and maintenance costs were considered to be dependent on the size of the FO installation. Specifically, the labour and maintenance costs accounted for 1% and 2.25% of the capital costs, respectively (Fritzmann et al., 2007; Vinardell et al., 2020a).

2.4.2 Draw solution replenishment costs

The draw solution needs to be replenished due to losses of draw solute through both FO and RO membranes. Draw solute losses through FO membranes were calculated for each solute using Eq. (2) (see Section 2.2), while the draw solute losses through RO membranes were calculated using the Reverse Osmosis System Analysis (ROSA) software (Filmtec Corporation, US). Detailed information of the input parameters to

ROSA can be found in Table S5 of the supplementary material. The purchase cost of each draw solute was obtained from Bacaksiz et al. (2021) and is reported in Table 1.

2.4.3 Energy production

The energy production was calculated considering a methane calorific value of 55 MJ kg^{-1} (Metcalf & Eddy, 2014). The produced methane was combusted in a CHP unit with electrical and thermal efficiencies of 33 and 55%, respectively (Riley et al., 2020; Vinardell et al., 2021). The capital and operating costs of the CHP unit were 712 € kW_{el}^{-1} and 0.0119 € kWh_{el}^{-1}, respectively (Riley et al., 2020). The lifetime of the CHP unit was considered to be 20 years (Whiting and Azapagic, 2014). The electricity produced in the CHP unit was considered to be sold at a price of 0.1283 € kWh^{-1} (Eurostat, 2021).

2.5 Economic evaluation

The capital expenditures (CAPEX), operating expenditures (OPEX) and electricity revenue were calculated for the different draw solutes and FO membranes. Eq. (5) and Eq. (6) were used to calculate the present value (PV) of the gross cost and electricity revenue, respectively. Subsequently, the PV of the net cost was calculated as the difference between the PV of the gross cost and the PV of the electricity revenue (Eq. (7)).

$$PV_{GC} = CAPEX + \sum_{t=1}^{T} \frac{OPEX_t}{(1+i)^t} \quad \text{Eq. (5)}$$

$$PV_{ER} = \sum_{t=1}^{T} \frac{ER_t}{(1+i)^t} \quad \text{Eq. (6)}$$

$$PV_{NC} = CAPEX + \sum_{t=1}^{T} \frac{OPEX_t - ER_t}{(1+i)^t} \quad \text{Eq. (7)}$$

where PV_{GC} is the PV of the gross cost (€), PV_{ER} is the PV of the electricity revenue (€), PV_{NC} is the PV of the net cost (€), CAPEX is the capital expenditure (€), $OPEX_t$ is the operating expenditure at year t (€), ER_t is the electricity revenue at year t (€), i is the discount rate (5%) and T is the plant lifetime (20 years).

3. Results and discussion

3.1 Impact of draw solute and membrane material on the economic balance of the FO+AnMBR system

Figure 2 illustrates the PV of the gross cost, electricity revenue and net cost for the different draw solutes and both membrane materials. The results show that the net cost of TFC membrane was substantially lower than the net cost of the CTA membrane regardless of the draw solute. The difference between both membranes can be mainly attributed to the higher water permeability and higher solute selectivity of TFC membrane in comparison with CTA membrane (Table 1). From these results, it is possible to conclude that the enhanced permselectivity (A/B ratio) (Shaffer et al., 2015) achieved with TFC membrane is an important factor influencing the economics of the process. The structural parameter (S), which relates to the properties of the membrane support layer, was lower for TFC membrane than for CTA membrane (Table 1). In this study, the membrane properties of the TFC membrane were obtained from Sanahuja-Embuena et al. (2019), who used a commercial Aquaporin membrane module and reported S values lower than commercial CTA membranes. Achieving a low S parameter is important to decrease the effect of ICP on the support layer and to increase the effective osmotic pressure difference between the draw and feed solutions (Blandin et al., 2015). These results illustrate that the improved properties of novel TFC membranes allowed increasing the water flux and reducing the draw solute flow rate through the FO

membranes, which had a direct impact on FO installation and draw solution replenishment costs. However, further research is necessary to better understand the impact of membrane material on the economic balance of the FO+AnMBR system by using other commercial CTA and TFC membranes.

The draw solute had a moderate impact on the economic balance of the FO+AnMBR system (Figure 2). Regarding CTA membrane, CH_3COONa and $CaCl_2$ were the most economically competitive draw solutes. CH_3COONa featured a slightly lower net cost than $CaCl_2$ despite the higher gross cost of CH_3COONa. This can be attributed to the higher electricity revenue achieved in the AnMBR when using CH_3COONa as draw solute since the fraction of CH_3COONa that permeates from the draw solution to the sewage through the FO membrane is converted into methane. The net cost of $MgCl_2$ and Na_2SO_4 were slightly higher than CH_3COONa and $CaCl_2$. Despite its relatively low FO membrane fluxes (~4.6 L m^{-2} h^{-1} ~~LMH~~), Na_2SO_4 was one of the most economically favourable draw solutes (Table 1). The good economic prospect of Na_2SO_4 can be attributed to the relatively low RSF of Na_2SO_4 through FO membranes (~2.5 g m^{-2} h^{-1}) that decreased the replenishment costs of the draw solute. However, the presence of sulphate in the pre-concentrated sewage decreases the amount of energy recovered in the AnMBR because of the competition between methanogens and sulphate reducing bacteria (SRB) for the available organic matter (Figure 2). Additionally, the higher concentration of sulphate in sewage increases the production of H_2S in the AnMBR that could (i) partially inhibit anaerobic microorganisms, (ii) increase the requirements for biogas desulphurisation and (iii) reduce the durability of the infrastructure and hinder the long-term operability of the AnMBR (out of the scope of the present study).

Figure 2 also shows that the economic balance of NaCl, $Ca(NO_3)_2$ and KCl was little attractive since these solutes featured the highest RSF (>4 g m^{-2} h^{-1}) despite achieving relatively high FO membrane fluxes (>5.7 L m^{-2} h^{-1}). This is particularly important for $Ca(NO_3)_2$ because high RSF increases the concentration of nitrate in the sewage that, in turn, decreases the amount of organic matter available for methane production (Figure 2). Furthermore, high RSFs could enhance biofouling and scaling on FO active layer due the interaction of the sewage compounds with the draw solute cations (i.e. Na^+, Ca^{2+}, Mg^{2+}) (She et al., 2012; Zou et al., 2019). These results illustrate that the selection of a suitable draw solute for FO+AnMBR system requires a compromise solution considering the capability of the draw solute to achieve high water fluxes with limited RSF.

Regarding TFC membrane, $MgCl_2$ was the most economically favourable draw solute followed by NaCl and $MgSO_4$ (Figure 2). This is in agreement with the net cost results obtained with CTA membrane since the same trend was observed for these three solutes. However, further experimental work is needed to expand the results of the TFC membrane by testing other draw solutes, such as KCl, $CaCl_2$, Na_2SO_4, $Ca(NO_3)_2$ and CH_3COONa. Finally, it is worth mentioning that $MgSO_4$ was not economically favourable for none of the membranes since this draw solute (i) featured a noticeably lower FO membrane flux in comparison to the other draw solutes and (ii) produced a limited amount of methane in the AnMBR due to the presence of sulphate in the pre-concentrated sewage.

3.2 Gross cost distribution

Figure 3 shows the gross cost distribution for the different draw solutes and both membranes. Regarding CTA membrane, the capital cost of the FO system represented the highest cost contributor (33-39%) for $MgCl_2$, $CaCl_2$, Na_2SO_4, $MgSO_4$ and CH_3COONa

(Figure 3B). The replacement of the FO membranes during the plant lifetime represented the second highest impact for these five draw solutes (31-37%). This shows that the costs associated with the FO installation had a high impact on the net cost for $MgCl_2$, $CaCl_2$, Na_2SO_4, $MgSO_4$ and CH_3COONa. Similar results were obtained for the TFC membrane since the FO capital cost (33-39%) and FO membrane replacement cost (31-36%) represented the two highest cost contributors for $MgCl_2$ and $MgSO_4$ (Figure 3B). However, in absolute values, the gross cost contribution of the costs related to FO installation (i.e. FO capital cost, FO membrane replacement cost, FO draw solution replenishment cost, maintenance cost and labour cost) were noticeably reduced when using the TFC membrane because of the better flux performance than CTA membrane (Figure 3A). These results highlight the importance of achieving high water permeabilities for the FO+AnMBR system.

The FO draw solution replenishment cost represented the highest cost contributor for CTA membrane using NaCl, KCl and $Ca(NO_3)_2$ (29-39%) as draw solutes (Figure 3B). The high impact of FO draw solution replenishment on the net cost for these three draw solutes can be attributed to: (i) the high RSF (>4 g m^{-2} h^{-1}), which increased the necessity to replenish the solute to keep the draw solute osmotic pressure constant and (ii) the higher water flux (>5.7 L m^{-2} h^{-1}) of these solutes, which minimised the contribution of FO installation to the net cost. The draw solution replenishment cost also represented the highest cost contributor for TFC membrane when using NaCl (32%) as draw solute (Figure 3B). However, in absolute values, the gross cost contributor of draw solution replenishment was also reduced with the TFC membrane because TFC membrane featured a lower RSF and a higher permselectivity than CTA membrane (Figure 3A). For

all draw solutes, the CHP capital and operating costs did not have a high impact on the net cost since their contribution was below 5% of the gross cost contribution.

3.3 Sensitivity analysis

Figure 4 illustrates the net cost of the different draw solutes and membranes for a ±30% variation of the most relevant economic parameters. The results show that the FO membrane cost variation had the highest impact on the net cost for all the draw solutes except for KCl (CTA membrane) and NaCl (TFC membrane). The variation of FO membrane cost affects both the initial investment and the cost to replace the FO membranes during the plant lifetime. These results highlight that FO membrane flux is a key economic driver in the FO+AnMBR system since this determines the FO membrane area required, which is directly correlated with the FO membrane purchasing and replacement cost. The variation of the FO membranes lifetime also had a high effect on the economic balance. This points out the importance to extend the lifetime of FO membranes to further improve the competitiveness of the system, which could be achieved by optimising the FO operational conditions and chemical cleaning strategy (Im et al., 2020). The chemical cost variation had the highest impact on the net cost for KCl and NaCl in CTA and TFC membranes, respectively (Figure 4). This can be directly attributed to the high RSF of these draw solutes for CTA and TFC membranes.

Figure 4 results also show that the electricity price variation led to small and moderate changes in the net cost for CTA and TFC membranes, respectively. For CTA, the impact of electricity price variation on net cost was nearly negligible for Na_2SO_4, $MgSO_4$ and $Ca(NO_3)_2$ since these solutes substantially decreased the production of methane in the AnMBR and made the electricity revenue irrelevant in comparison to the other cost contributors. Conversely, the impact of the electricity price variation on the net cost was

408 relatively high when using CH_3COONa as a draw solute since this solute increased the
409 methane production in the AnMBR. The electricity price variation had a higher impact
410 on the TFC economic balance since (i) the methane production is similar regardless of
411 the type of FO membrane used and (ii) the FO-related costs are lower for TFC than for
412 CTA membranes. These results imply that the superior performance of the TFC
413 membranes makes the relative importance of electricity revenue higher for TFC
414 membranes than for CTA membranes.

415 **3.4 Impact of draw solute on permeate quality and AnMBR performance**

416 Table 2 shows the COD concentration (both influent and permeate), draw solute
417 concentration and methane production of the AnMBR for the different draw solutes,
418 membrane materials and FO recoveries. Besides the 80% FO recovery used in the
419 previous sections, this section included two additional FO recoveries (i.e. 50 and 90%) to
420 better understand the impact of sewage pre-concentration on the AnMBR performance
421 (i.e. methane production and permeate quality).

422 Table 2 results show that the AnMBR COD removal efficiency was similar regardless of
423 the draw solute and FO membrane material since the permeate COD concentration
424 remained rather constant at a specific FO recovery condition. These results indicate that,
425 despite the sewage pre-concentration and RSF, inhibition of the anaerobic biomass would
426 have a minor impact on AnMBR performance (Table 2). Besides the great adaptability of
427 anaerobic biomass to operate under harsh conditions, the slight loss of activity due to
428 inhibition could be mitigated by increasing the concentration of active biomass in the
429 AnMBR (Chen et al., 2008). The loss of activity could also be mitigated by the capability
430 of the AnMBR to retain specific microorganisms able to tolerate higher inhibitory

concentrations regardless of their doubling time and aggregation properties (Dereli et al., 2012; Puyol et al., 2017).

Methane production was similar for NaCl, $MgCl_2$, KCl and $CaCl_2$ regardless of the FO membrane material and FO recovery (Table 2). However, methane production substantially decreased when using Na_2SO_4, $MgSO_4$ and $Ca(NO_3)_2$ as draw solutes since these solutes decreased the amount of organic matter available for methanisation. For these draw solutes, the amount of methane produced progressively decreased as the FO recovery increased due to the higher concentration of draw solute in the pre-concentrated sewage at higher FO recoveries. This was particularly noticeable for $Ca(NO_3)_2$ since the RSF of $Ca(NO_3)_2$ was substantially higher than $MgSO_4$ and Na_2SO_4. Accordingly, the high presence of nitrate in the pre-concentrated sewage sharply decreased methane production at FO recoveries of 80 and 90%. CH_3COONa achieved the highest methane production among the different draw solutes because this draw solute increased the amount of easily biodegradable organic matter in the pre-concentrated sewage, which allowed maximising methane production in the AnMBR.

Increasing the pre-concentration factor has a direct impact on AnMBR permeate quality. The permeate COD concentration increased as the FO recovery increased, increasing both the concentration of biodegradable organic matter (S_S) and the concentration of soluble inerts (S_I). This phenomenon was particularly important for the high FO recovery scenarios (80 and 90%) since the permeate COD concentration could exceed the European Union COD discharge limits (<125 mg COD L^{-1}) (CEC, 1991). Additionally, the nitrogen and phosphorus concentrations in the permeate also increase with the FO recovery. For this reason, the implementation of post-treatments would be necessary to

meet the effluent discharge limits for COD and nutrients when FO and AnMBR technologies are combined.

The draw solute concentration also increased with the FO recovery. For the CTA membrane, the NaCl concentration increased from 0.65 to 5.89 mg L^{-1} as the FO recovery increased from 50 to 90% (Table 2). However, the NaCl concentration in the pre-concentrated sewage was substantially decreased using TFC membrane due to its higher permselectivity. Compared to the CTA membrane, TFC membrane decreased the NaCl, $MgCl_2$ and $MgSO_4$ concentrations in the pre-concentrated sewage by 3, 8 and 11 times, respectively (Table 2). These results indicate that high FO recoveries could result in a permeate and digestate with a high salinity concentration, which could limit their application in agriculture as irrigation water and fertilizers (Vinardell et al., 2021). The production of digestates with high salinities would make necessary to apply other management alternatives such as incineration or landfilling. Accordingly, restricting the FO recovery could be used as a strategy to (i) meet the effluent discharge requirements and (ii) improve the quality of the permeate and digestate to make it suitable for agricultural application. These two factors are paramount to make the FO+AnMBR approach environmentally and technically feasibility.

4. Conclusions

The techno-economic analysis of the FO+AnMBR system showed that FO membrane material was a determinant economic factor since the net cost of the TFC membrane was substantially lower than the CTA membrane. The draw solute had a moderate impact on the FO+AnMBR system economic balance. The capital cost of the FO system was the most important cost contributor for $MgCl_2$, $CaCl_2$, Na_2SO_4, $MgSO_4$ and CH_3COONa (33-

39%), whereas ~~while~~ the FO draw solution replenishment was the most important cost contributor for NaCl, KCl and $Ca(NO_3)_2$ (29-32%). The most economically favourable draw solutes were CH_3COONa and $CaCl_2$ for the CTA membrane and $MgCl_2$ for the TFC membrane due to their capacity to achieve relatively high water fluxes with low RSF. The AnMBR COD removal efficiency (>90%) was similar regardless of the draw solute and membrane material. However, FO recoveries above 80% could compromise the fulfilment of the permeate discharge requirements. Future experimental research using different commercial CTA/TFC FO membranes and draw solutes is needed to expand and complement the results obtained in the present study. Overall, the results from this techno-economic study highlight that selecting FO membranes and draw solutes capable to achieve high water fluxes with reduced RSF is crucial to boost the economic competitiveness of the system and fulfil the permeate discharge requirements.

Acknowledgments

This work was supported by the European Union LIFE programme (LIFE Green Sewer project, LIFE17 ENV/ES/000341). The authors also acknowledge the grant overseen by the French National Research Agency (ANR) as part of the "JCJC" Program BàMAn (ANR-18-CE04-0001-01). Sergi Vinardell is grateful to the Generalitat de Catalunya for his predoctoral FI grant (2019 FI_B 00394). Sergi Astals is grateful to the Spanish Ministry of Science, Innovation and Universities for his Ramon y Cajal fellowship (RYC-2017-22372). Gaetan Blandin received the support of a fellowship from "la Caixa" Foundation (ID 100010434). The fellowship code is LCF/BQ/PR21/11840009. Finally, the authors would like to thank the Catalan Government for the quality accreditation given to Environmental Biotechnology research group (2017 SGR 1218).

Declaration of competing interests

The authors declare that they have no known competing financial interests or personal relationships that could have appeared to influence the work reported in this paper. The authors also declare that this manuscript reflects only the authors' view and that the Executive Agency for SME/EU Commission are not responsible for any use that may be made of the information it contains.

References

Achilli, A., Cath, T.Y., Childress, A.E., 2010. Selection of inorganic-based draw solutions for forward osmosis applications. J. Memb. Sci. 364, 233–241.

Almoalimi, K., Liu, Y.-Q., 2022. Enhancing ammonium rejection in forward osmosis for wastewater treatment by minimizing cation exchange. J. Memb. Sci. 648, 120365.

Anjum, F., Khan, I.M., Kim, J., Aslam, M., Blandin, G., Heran, M., Lesage, G., 2021. Trends and progress in AnMBR for domestic wastewater treatment and their impacts on process efficiency and membrane fouling. Environ. Technol. Innov. 21, 101204.

Ansari, A.J., Hai, F.I., Guo, W., Ngo, H.H., Price, W.E., Nghiem, L.D., 2015. Selection of forward osmosis draw solutes for subsequent integration with anaerobic treatment to facilitate resource recovery from wastewater. Bioresour. Technol. 191, 30–36.

Ansari, A.J., Hai, F.I., Price, W.E., Drewes, J.E., Nghiem, L.D., 2017. Forward osmosis as a platform for resource recovery from municipal wastewater - A critical assessment of the literature. J. Memb. Sci. 529, 195–206.

Ansari, A.J., Hai, F.I., Price, W.E., Ngo, H.H., Guo, W., Nghiem, L.D., 2018. Assessing the integration of forward osmosis and anaerobic digestion for simultaneous

wastewater treatment and resource recovery. Bioresour. Technol. 260, 221–226.

Arcanjo, G.S., Costa, F.C.R., Ricci, B.C., Mounteer, A.H., de Melo, E.N.M.L., Cavalcante, B.F., Araújo, A. V., Faria, C. V., Amaral, M.C.S., 2020. Draw solution solute selection for a hybrid forward osmosis-membrane distillation module: Effects on trace organic compound rejection, water flux and polarization. Chem. Eng. J. 400, 125857.

Ariesyady, H.D., Ito, T., Okabe, S., 2007. Functional bacterial and archaeal community structures of major trophic groups in a full-scale anaerobic sludge digester. Water Res. 41, 1554–1568.

Awad, A.M., Jalab, R., Minier-Matar, J., Adham, S., Nasser, M.S., Judd, S.J., 2019. The status of forward osmosis technology implementation. Desalination 461, 10–21.

Bacaksiz, A.M., Kaya, Y., Aydiner, C., 2021. Techno-economic preferability of cost-performance effective draw solutions for forward osmosis and osmotic anaerobic bioreactor applications. Chem. Eng. J. 410, 127535.

Blandin, G., Galizia, A., Monclús, H., Lesage, G., Héran, M., Martinez-Lladó, X., 2021. Submerged osmotic processes: Design and operation of hollow fiber forward osmosis modules. Desalination 518, 115281.

Blandin, G., Verliefde, A.R.D., Tang, C.Y., Le-Clech, P., 2015. Opportunities to reach economic sustainability in forward osmosis–reverse osmosis hybrids for seawater desalination. Desalination 363, 26–36.

Cabrera-Castillo, E.H., Castillo, I., Ciudad, G., Jeison, D., Ortega-Bravo, J.C., 2021. FO-MD setup analysis for acid mine drainage treatment in Chile: An experimental-

544 theoretical economic assessment compared with FO-RO and single RO.
545 Desalination 514, 115164.

546 CEC, 1991. Council Directive of 21 May 1991 concerning waste water treatment
547 (91/271/EEC). Off. J. Eur. Communities No. L 135/40-52.

548 Chen, Y., Cheng, J.J., Creamer, K.S., 2008. Inhibition of anaerobic digestion process: A
549 review. Bioresour. Technol. 99, 4044-4064.

550 Coday, B.D., Heil, D.M., Xu, P., Cath, T.Y., 2013. Effects of transmembrane hydraulic
551 pressure on performance of forward osmosis membranes. Environ. Sci. Technol. 47,
552 2386–2393.

553 Dereli, R.K., Ersahin, M.E., Ozgun, H., Ozturk, I., Jeison, D., van der Zee, F., van Lier,
554 J.B., 2012. Potentials of anaerobic membrane bioreactors to overcome treatment
555 limitations induced by industrial wastewaters. Bioresour. Technol. 122, 160–170.

556 Eurostat, 2021. Electricity price statistics. https://ec.europa.eu/eurostat/statistics-
557 explained/index.php?title=Electricity_price_statistics#Electricity_prices_for_non-
558 household_consumers. (accessed 8 March, 2022).

559 Ferby, M., Zou, S., He, Z., 2020. Reduction of reverse solute flux induced solute buildup
560 in the feed solution of forward osmosis. Environ. Sci. Water Res. Technol. 6, 423–
561 435.

562 Ferrari, F., Balcazar, J.L., Rodriguez-Roda, I., Pijuan, M., 2019. Anaerobic membrane
563 bioreactor for biogas production from concentrated sewage produced during sewer
564 mining. Sci. Total Environ. 670, 993–1000.

565 Fritzmann, C., Löwenberg, J., Wintgens, T., Melin, T., 2007. State-of-the-art reverse

566 osmosis desalination. Desalination 216, 1–76.

567 Hu, Y., Du, R., Nitta, S., Ji, J., Rong, C., Cai, X., Qin, Y., Li, Y.Y., 2021. Identification
568 of sustainable filtration mode of an anaerobic membrane bioreactor for wastewater
569 treatment towards low-fouling operation and efficient bioenergy production. J.
570 Clean. Prod. 329.

571 Im, S.J., Jeong, Sanghyun, Jeong, Seongpil, Jang, A., 2020. Techno-economic evaluation
572 of an element-scale forward osmosis-reverse osmosis hybrid process for seawater
573 desalination. Desalination 476, 114240.

574 Irvine, G.J., Rajesh, S., Georgiadis, M., Phillip, W.A., 2013. Ion selective permeation
575 through cellulose acetate membranes in forward osmosis. Environ. Sci. Technol. 47,
576 13745–13753.

577 Kim, J.E., Phuntsho, S., Chekli, L., Hong, S., Ghaffour, N., Leiknes, T.O., Choi, J.Y.,
578 Shon, H.K., 2017. Environmental and economic impacts of fertilizer drawn forward
579 osmosis and nanofiltration hybrid system. Desalination 416, 76–85.

580 Kim, M. kyu, Chang, J.W., Park, K., Yang, D.R., 2022. Comprehensive assessment of
581 the effects of operating conditions on membrane intrinsic parameters of forward
582 osmosis (FO) based on principal component analysis (PCA). J. Memb. Sci. 641,
583 119909.

584 Krzeminski, P., Leverette, L., Malamis, S., Katsou, E., 2017. Membrane bioreactors – A
585 review on recent developments in energy reduction, fouling control, novel
586 configurations, LCA and market prospects. J. Memb. Sci. 527, 207–227.

587 Lutchmiah, K., Verliefde, A.R.D., Roest, K., Rietveld, L.C., Cornelissen, E.R., 2014.

588 Forward osmosis for application in wastewater treatment: A review. Water Res. 58,
589 179-197.

590 Maaz, M., Yasin, M., Aslam, M., Kumar, G., Atabani, A.E., Idrees, M., Anjum, F., Jamil,
591 F., Ahmad, R., Khan, A.L., Lesage, G., Heran, M., Kim, J., 2019. Anaerobic
592 membrane bioreactors for wastewater treatment: Novel configurations, fouling
593 control and energy considerations. Bioresour. Technol. 283, 358–372.

594 Metcalf & Eddy, 2014. Wastewater Engineering: Treatment and Resource Recovery.
595 Fifth ed. McGraw Hill, New York.

596 Puyol, D., Batstone, D.J., Hülsen, T., Astals, S., Peces, M., Krömer, J.O., 2017. Resource
597 recovery from wastewater by biological technologies: Opportunities, challenges,
598 and prospects. Front. Microbiol. 7.

599 Riley, D.M., Tian, J., Güngör-Demirci, G., Phelan, P., Rene Villalobos, J., Milcarek, R.J.,
600 2020. Techno-economic assessment of CHP systems in wastewater treatment plants.
601 Environments 7, 1–32.

602 Sanahuja-Embuena, V., Khensir, G., Yusuf, M., Andersen, M.F., Nguyen, X.T.,
603 Trzaskus, K., Pinelo, M., Helix-Nielsen, C., 2019. Role of operating conditions in a
604 pilot scale investigation of hollow fiber forward osmosis membrane modules.
605 Membranes. 9, 66.

606 Shaffer, D.L., Werber, J.R., Jaramillo, H., Lin, S., Elimelech, M., 2015. Forward osmosis:
607 Where are we now? Desalination 356, 271–284.
608 https://doi.org/10.1016/j.desal.2014.10.031

609 She, Q., Jin, X., Li, Q., Tang, C.Y., 2012. Relating reverse and forward solute diffusion

610 to membrane fouling in osmotically driven membrane processes. Water Res. 46,
611 2478–2486.

612 Tiraferri, A., Yip, N.Y., Straub, A.P., Romero-Vargas Castrillon, S., Elimelech, M., 2013.
613 A method for the simultaneous determination of transport and structural parameters
614 of forward osmosis membranes. J. Memb. Sci. 444, 523–538.

615 Valladares Linares, R., Li, Z., Yangali-Quintanilla, V., Ghaffour, N., Amy, G., Leiknes,
616 T., Vrouwenvelder, J.S., 2016. Life cycle cost of a hybrid forward osmosis – low
617 pressure reverse osmosis system for seawater desalination and wastewater recovery.
618 Water Res. 88, 225–234.

619 Vinardell, S., Astals, S., Jaramillo, M., Mata-Alvarez, J., Dosta, J., 2021. Anaerobic
620 membrane bioreactor performance at different wastewater pre-concentration factors:
621 An experimental and economic study. Sci. Total Environ. 750, 141625.

622 Vinardell, S., Astals, S., Mata-Alvarez, J., Dosta, J., 2020a. Techno-economic analysis of
623 combining forward osmosis-reverse osmosis and anaerobic membrane bioreactor
624 technologies for municipal wastewater treatment and water production. Bioresour.
625 Technol. 297, 122395.

626 Vinardell, S., Astals, S., Peces, M., Cardete, M.A., Fernández, I., Mata-Alvarez, J., Dosta,
627 J., 2020b. Advances in anaerobic membrane bioreactor technology for municipal
628 wastewater treatment: A 2020 updated review. Renew. Sustain. Energy Rev. 130,
629 109936.

630 Wang, J., Liu, X., 2021. Forward osmosis technology for water treatment: Recent
631 advances and future perspectives. J. Clean. Prod. 280, 124354.

Whiting, A., Azapagic, A., 2014. Life cycle environmental impacts of generating electricity and heat from biogas produced by anaerobic digestion. Energy 70, 181–193.

Yangali-Quintanilla, V., Olesen, L., Lorenzen, J., Rasmussen, C., Laursen, H., Vestergaard, E., Keiding, K., 2015. Lowering desalination costs by alternative desalination and water reuse scenarios. Desalin. Water Treat. 55, 2437–2445.

Zahedi, S., Ferrari, F., Blandin, G., Balcazar, J.L., Pijuan, M., 2021. Enhancing biogas production from the anaerobic treatment of municipal wastewater by forward osmosis pretreatment. J. Clean. Prod. 315, 128140.

Zhang, X., Liu, Y., 2022. Circular economy is game-changing municipal wastewater treatment technology towards energy and carbon neutrality. Chem. Eng. J. 429, 132114.

Zhen, G., Pan, Y., Lu, X., Li, Y.-Y., Zhang, Z., Niu, C., Kumar, G., Kobayashi, T., Zhao, Y., Xu, K., 2019. Anaerobic membrane bioreactor towards biowaste biorefinery and chemical energy harvest: Recent progress, membrane fouling and future perspectives. Renew. Sustain. Energy Rev. 115, 109392.

Zou, S., Qin, M., He, Z., 2019. Tackle reverse solute flux in forward osmosis towards sustainable water recovery: reduction and perspectives. Water Res. 149, 362–374.

Table 1. A, B and S parameters as well as main properties and costs for the different draw solutes and membranes under study.

	CTA Membrane								TFC Membrane		
	NaCl	**$MgCl_2$**	**KCl**	**$CaCl_2$**	**Na_2SO_4**	**$MgSO_4$**	**$Ca(NO_3)_2$**	**CH_3COONa**	**NaCl**	**$MgCl_2$**	**$MgSO_4$**
A ($L\ m^{-2}\ h^{-1}\ bar^{-1}$)[a]	0.55	0.55	0.55	0.55	0.55	0.55	0.55	0.55	1.71	1.71	1.71
S (mm)[a]	0.463	0.463	0.463	0.463	0.463	0.463	0.463	0.463	0.14	0.14	0.14
B ($L\ m^{-2}\ h^{-1}$)[b]	0.303	0.215	0.363	0.268	0.091	0.04	0.15	0.073	0.240	0.07	0.01
D ($\times 10^{-9}\ m^2\ s^{-1}$)[c]	1.47	1.05	1.86	1.13	0.76	0.37	1.28	1.44	1.47	1.05	0.37
k ($\times 10^{5}\ m\ s^{-1}$)[d]	1.99	1.59	2.32	1.67	1.28	0.79	1.81	1.96	1.99	1.59	0.79
Initial osmotic pressure (bar)	28	28	28	28	28	28	28	28	28	28	28
Initial draw solute concentration ($g\ L^{-1}$)[e]	35.2	34.2	47.0	43.8	84.7	141.3	87.2	55.9	35.2	34.2	141.3
Cation concentration ($g\ L^{-1}$)	13.8	8.7	24.7	15.8	27.4	28.5	21.3	15.7	13.8	8.7	28.5
Anion concentration ($g\ L^{-1}$)	21.4	25.5	22.3	28.0	57.3	112.8	65.9	40.2	21.4	25.5	112.8
Draw solute purchase cost (€ mol^{-1})[f]	0.016	0.025	0.020	0.015	0.013	0.017	0.038	0.034	0.016	0.025	0.017

[a] Coday et al. (2013) for CTA membrane and Sanahuja-Embuena et al. (2019) for TFC membrane.

[b] Calculated from data provided by Achilli et al. (2010) and Ansari et al. (2015) for CTA membrane and Sanahuja-Embuena et al. (2019) for TFC membrane.

[c] Achilli et al. (2010) for NaCl, $MgCl_2$, KCl, $CaCl_2$, Na_2SO_4 and $MgSO_4$, Irvine et al. (2013) for $Ca(NO_3)_2$ and Ansari et al. (2015) for CH_3COONa.

[d] The k parameter was calculated from Sanahuja-Embuena et al. (2019) equations and parameters.

[e] Achilli et al. (2010) for NaCl, $MgCl_2$, KCl, $CaCl_2$, Na_2SO_4, $MgSO_4$ and $Ca(NO_3)_2$ and calculated from data provided by Arcanjo et al. (2020) for CH_3COONa.

[f] Data obtained from Bacaksiz et al. (2021).

Table 2. AnMBR performance and permeate quality for the different draw solutes and membranes under study. The AnMBR performance was modelled for an FO recovery of 50, 80 and 90%.

		CTA Membrane								TFC Membrane		
		NaCl	**$MgCl_2$**	**KCl**	**$CaCl_2$**	**Na_2SO_4**	**$MgSO_4$**	**$Ca(NO_3)_2$**	**CH_3COONa**	**NaCl**	**$MgCl_2$**	**$MgSO_4$**
R=50%	Influent COD concentration (mg L^{-1})	840	840	840	840	840	840	840	929	840	840	840
	Influent solute concentration (g L^{-1})	0.65	0.47	1.02	0.73	0.55	0.45	0.88	0.29	0.19	0.06	0.04
	Permeate COD concentration (mg L^{-1})	83.0	83.7	84.4	83.6	82.7	83.3	83.3	91.1	82.4	82.3	82.2
	Methane production (Nm^3 d^{-1})	10,992	10,991	10,989	10,991	6,621	6,790	3,462	14,927	10,993	10,993	10,617
	Electricity production (kWh d^{-1})	39,968	38,964	39,960	39,964	24,076	24,690	12,589	54,278	39,971	39,9971	38,604
R=80%	Influent COD concentration (mg L^{-1})	2,100	2,100	2,100	2,100	2,100	2,100	2,100	2,454	2,100	2,100	2,100
	Influent solute concentration (g L^{-1})	2.61	1.88	4.07	2.93	2.20	1.80	3.53	1.16	0.78	0.23	0.16
	Permeate COD concentration (mg L^{-1})	176.5	179.4	182.7	179.2	175.3	177.7	178.0	189.5	173.9	173.6	173.2
	Methane production (Nm^3 d^{-1})	11,745	11,743	11,742	11,744	4,753	5,023	0	18,053	11,747	11,747	11,145
	Electricity production (kWh d^{-1})	42,708	42,702	42,696	42,703	17,281	18,263	0	65,643	42,713	42,713	40,526
R=90%	Influent COD concentration (mg L^{-1})	4,200	4,200	4,200	4,200	4,200	4,200	4,200	4,998	4,200	4,200	4,200
	Influent solute concentration (g L^{-1})	5.89	4.22	9.16	6.58	4.96	4.04	7.93	2.60	1.75	0.52	0.36
	Permeate COD concentration (mg L^{-1})	331.6	338.8	347.3	338.3	328.9	334.7	335.3	344.8	325.5	324.8	324.0
	Methane production (Nm^3 d^{-1})	11,996	11,994	11,993	11,995	4,130	4,433	0	19,096	11,998	11,998	11,321
	Electricity production (kWh d^{-1})	43,621	43,614	43,608	43,615	15,016	16,121	0	69,438	43,627	43,627	41,166

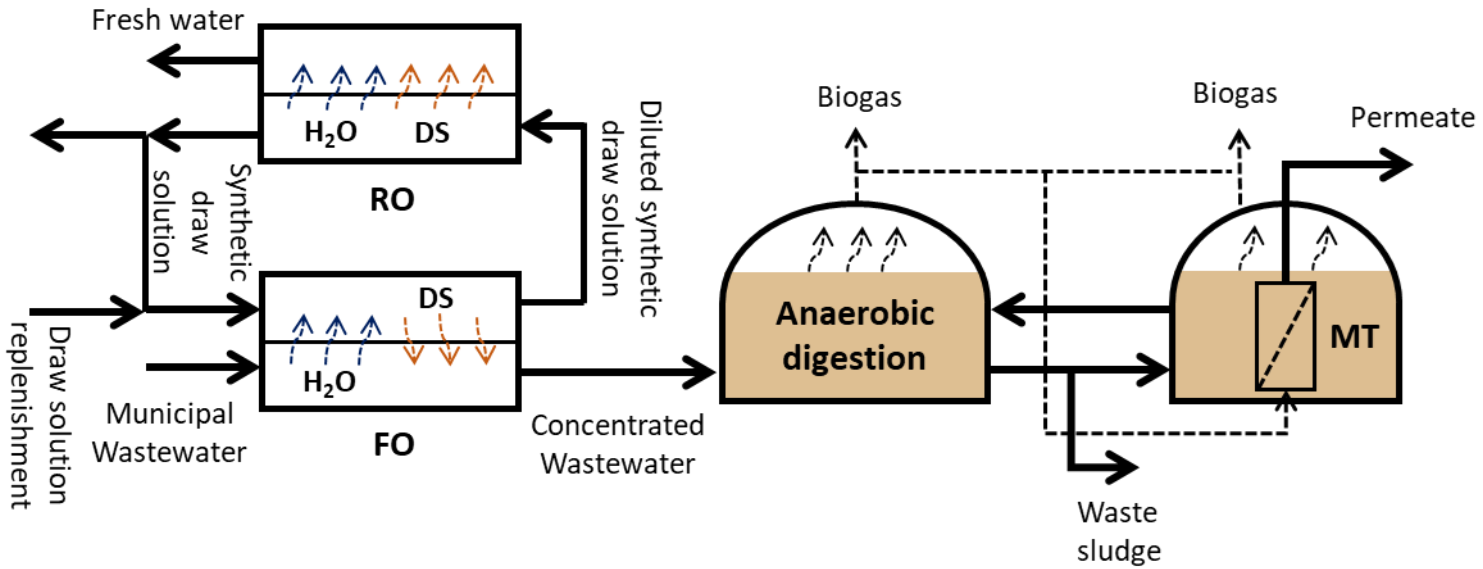

Figure 1. Closed-loop configuration integrating FO, RO and AnMBR technologies for municipal sewage treatment and water production (adapted from Vinardell et al. (2020a)).

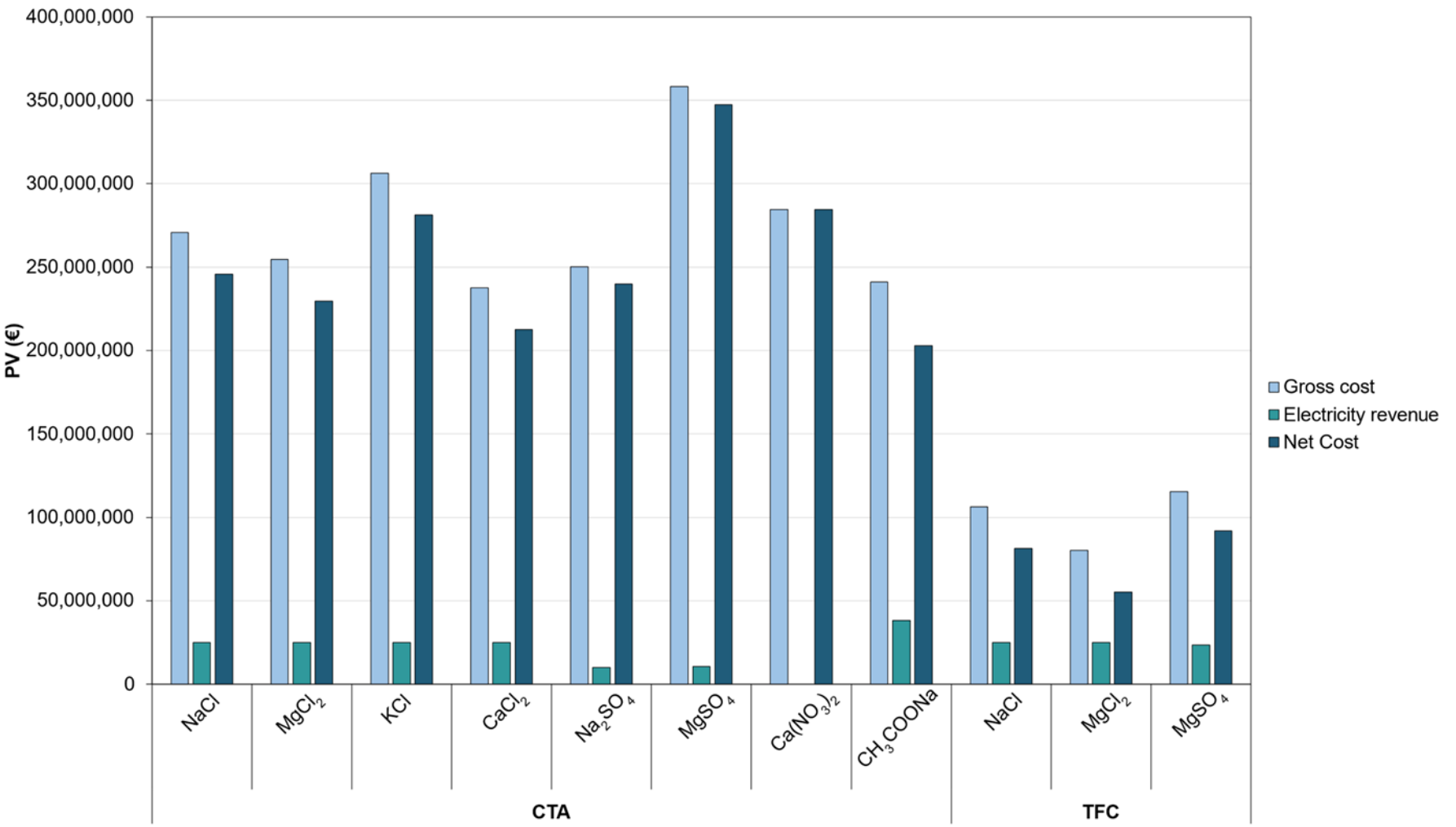

Figure 2. Present value (PV) of the gross cost, electricity revenue and net cost for the different draw solutes and membranes under study.

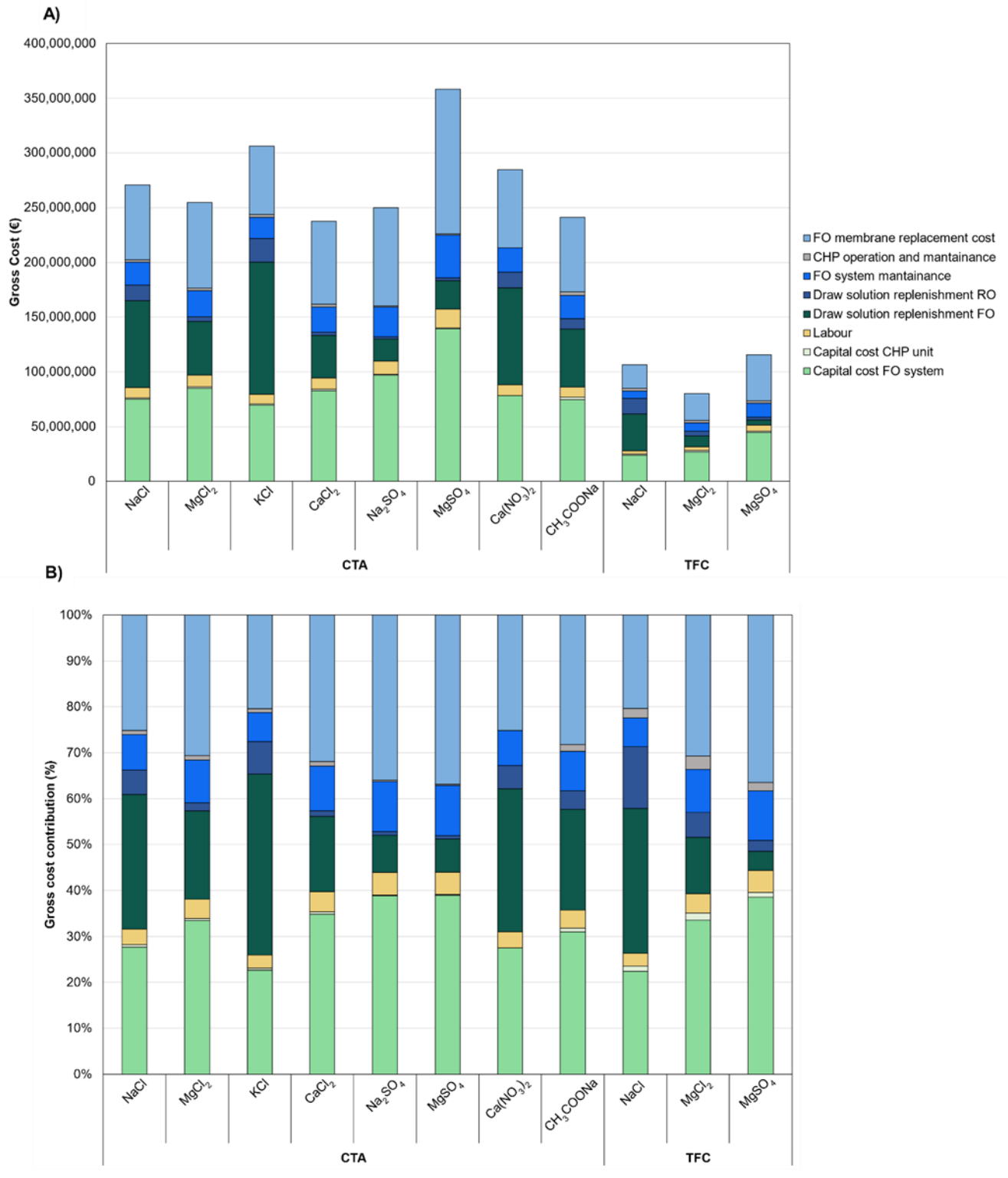

Figure 3. Gross cost contribution for the different draw solutes and membranes under study. (A) Absolute gross costs distribution (€); (B) relative gross cost distribution (%).

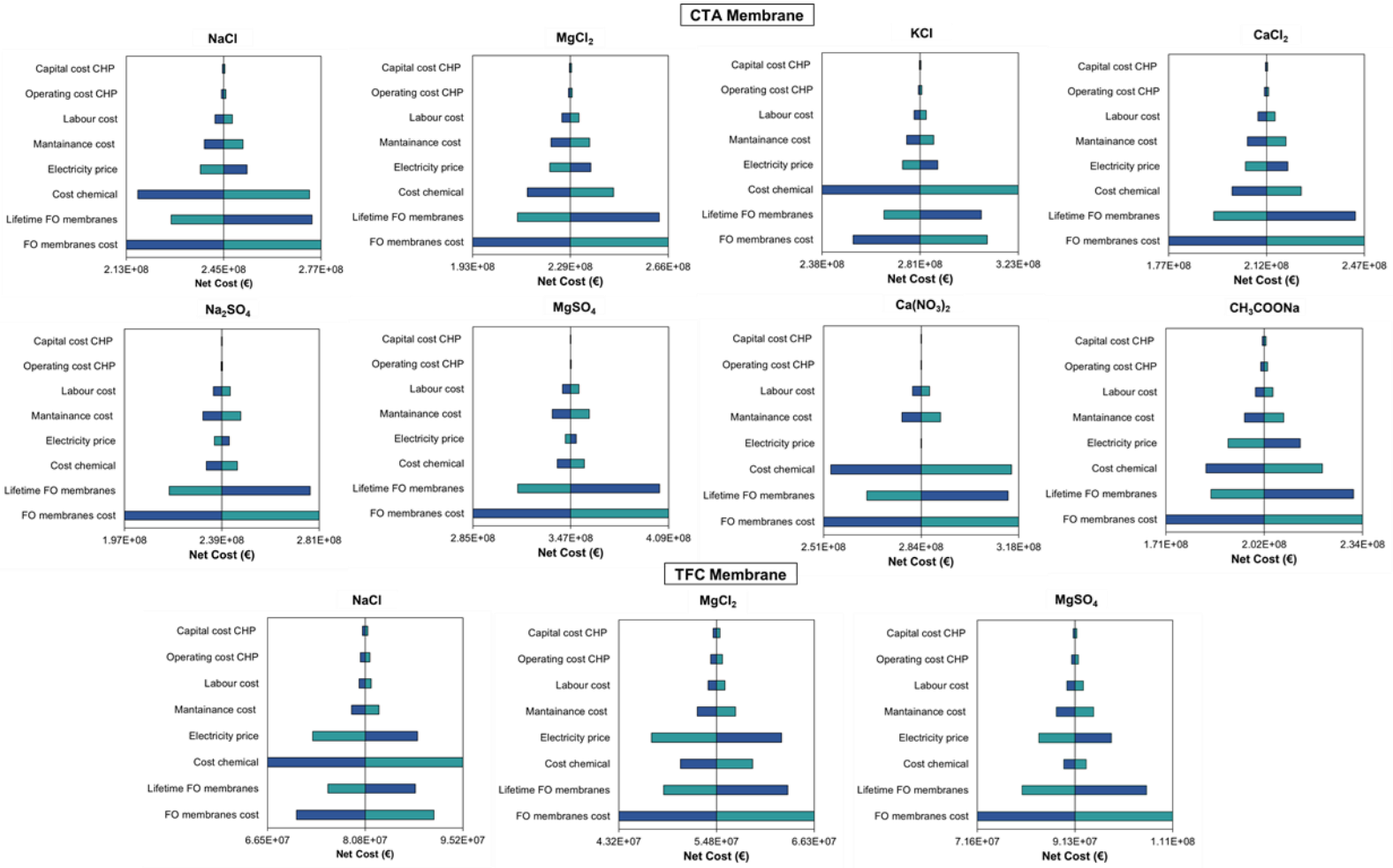

Figure 4. Sensitivity analysis of the net cost for a ±30% variation of the most important economic parameters for the different draw solutes and membranes under study.